JOURNAL OF SOLID STATE CHEMISTRY 86, 263–274 (1990)

Raman and X-Ray Diffraction Study of Boehmite Gels and Their Transformation to α- or β-Alumina

G. MARIOTTO AND E. CAZZANELLI

Dipartimento di Fisica, Università di Trento, 38050 Povo, Trento, Italy

AND G. CARTURAN, R. DI MAGGIO, AND P. SCARDI

Dipartimento di Ingegneria, Università di Trento, 38050 Mesiano, Trento, Italy

Received July 10, 1989; in revised form January 22, 1990

The structural evolution of gel-derived boehmite and alkali-doped boehmite samples, undergoing different heat treatments up to 1200°C, was followed by both X-ray diffraction and Raman scattering measurements, collected at room temperature. Our observations reveal the presence of different transition alumina phases at intermediate temperatures, before formation at the highest temperatures of stable α-alumina or $\beta + \beta''$-alumina, for alkali-loaded Al_2O_3. In particular, Raman data from samples treated at 400°C are consistent with a phase change from pseudo-boehmite to the γ-alumina structure, while the dehydroxylation process is not yet completed. The process appears independent of the presence of alkali: identical evolution was presented up to 800°C by all our samples. After final annealing at 1200°C the presence of alkali induces the formation of stable $\beta + \beta''$-alumina phases whereas, in the absence of alkali, a phase identified as Θ-Al_2O_3 is observed at 1000°C and, finally, stable α-Al_2O_3 is obtained at 1200°C.

1. Introduction

The unique features of sodium β- and β''-aluminas [mechanical strength, chemical stability, no electronic conductivity, but quite good ion mobility at moderate temperatures (*1*)] make these ceramics the most promising materials as solid electrolytes in the Na/S battery (*2*). Their ionic conductivity depends on production and processing methods (*3*), the achievement of β- and β''-aluminas with improved conductivity still being an intriguing challenge. With the aim of bypassing conventional preparation (*4*), new methods have been reported for processing β-alumina-type ceramics (*5*); among others, the sol-gel route seems a suitable approach (*6*, *7*), owing to the high purity of the material and morphology control of the final products.

These studies are related to sol-gel preparation of functional α-alumina ceramics (*8*, *9*), in which the most important factor is thermal evolution of the parent gel which, via topotactical occurrence of different transition phases, at high temperatures collapses by reconstructive transformation to α-alumina.

This topic is quite attractive, as revealed by the flourishing literature, in which com-

0022-4596/90 $3.00

pelling evidence, based on analysis with different techniques (*10–19*), definitely demonstrates the sensitivity of the final product to the experimental conditions used during production. In a recent paper (*20*) it has indirectly been suggested that β-$Al_2O_3 \cdot H_2O$ (diaspore), once obtained by sol-gel, may be the only intermediate phase leading to high-density formation of α-Al_2O_3 at low temperatures (*21, 22*).

Thus, sol-gel preparation of diaspore and β-β'' aluminas, to be used for seeding of α-aluminas (*20, 23*), encompasses efforts to improve the ion conductivity of final products as well the search for a suitable approach to low-temperature formation of high-density α-Al_2O_3.

This paper reports the concomitant evolution of some gels, containing either Al_2O_3 alone or combined with sodium or potassium oxide, which, under the same thermal conditions, gives α-alumina and Na or K $\beta + \beta''$-alumina, respectively, as final phases. For each significant step in this evolution an X-ray diffraction (XRD) study and a parallel Raman spectroscopic investigation were performed. It is worth remarking that slight modifications in chemical composition, symmetry of the basic molecular units, and the overall degree of order in gel-derived aluminas can be revealed by the Raman spectra (*24*), while X-ray diffraction patterns are directly related to both crystalline phases and sizes of crystallites at the different heat treatment temperatures (*18*). In the last few years, Raman spectroscopy has been extensively used both to follow the evolution of silica gels toward the glass state (*25–27*) and to monitor successfully the degree of order in β-alumina crystals, through linewidth analysis of vibrational modes in crystals with different composition (*28*). Of course, it can also give useful insights on the local symmetry of atom groups (*29*), not directly revealed by straightforward XRD analysis (*30*).

2. Experimental

2.1. Sample Preparation

A nearly transparent gel of Al_2O_3 was prepared following the method developed by Yoldas (*31*). In a typical experiment the hydrolysis of aluminum isopropoxide was performed by introducing the alkoxide into excess water (100 mole of H_2O per mole of alkoxide) at 80°C. After 30 min under stirring, a small quantity of HNO_3 (0.1 mole per mole of alkoxide) was added and the system was then left at 100–110°C for 1 day, to form a sol. This sol was divided into three parts which underwent different treatments.

One part was dried for 24 hr at 95°C, producing a transparent gel of Al_2O_3.

A titered solution of sodium methoxide was added to the second part to reach Na^+/Al^{3+} molar ratio = 1/6. The resulting mixture was stirred at room temperature for 1 day to ensure good homogeneity.

Analogously, potassium methoxide was added to the third part up to K^+/Al^{3+} molar ratio = 1/6, then stirred at room temperature for 24 hr.

The three gels were then dried at 170°C for 15 hr, in order to eliminate organic components and free water.

Gel samples of each composition were treated in turn at 400, 600, 800, 1000, and 1200°C, respectively, by keeping them for 2 hr in an oven, preset and stabilized at the desired temperature.

2.2. X-Ray Diffraction Experiments

X-ray measurements were performed on powdered samples on a Rigaku D/max B diffractometer equipped with a scintillation counter and a graphite curved crystal monochromator in the diffracted beam. Each measurement was carried out at 2°/min with steps of 0.02° in the range $20° \leq 2\Theta \leq 70°$, except for the boehmite samples for which the scanning speed was 1°/min. A

Casio 6000 computer, interfaced to the diffractometer, was employed for data processing and routine operations. For phase identification a search-match program, supported by JCPDS cards (*32*), was used as well as the diffraction patterns obtained from two standards of β- and β''-alumina (*33*). Peak separation and profile analysis were carried out only for the samples heated at 170°C, whose crystallite-size was evaluated using line broadening analysis through the Warren–Auerbach method (*34*).

2.3 Raman Scattering Measurements

Raman spectra were collected from small compact grains irregularly shaped, almost colorless, and typically 2–3 mm in size. Samples were annealed at the various temperatures just before being placed in an optical air-evacuated cryostat. Raman measurements were carried out at room temperature under excitation of a CW Ar^+ ion laser operating in turn at 514.5 and 488.0 nm, with an output power of about 300 mW in both cases. The scattered light was analyzed in a 90° geometry with a double monochromator equipped with holographic gratings; standard photon counting electronics was used for its detection. All measurements were performed with an instrumental resolution of 2.8 cm^{-1}, and the data were stored in a multichannel analyzer. The spectra turned out to be fully unpolarized due to the polycrystalline nature of our samples, which did not allow any polarization analysis of Raman scattering. Although specific features were sometimes sample-dependent, the main spectral shapes could be reproduced well for samples treated in the same way.

All samples dried for 15 hr at 170°C gave very good Raman spectra in the range 10–2000 cm^{-1}. They were superimposed upon a relatively weak and apparently flat luminescence background, the intensity of which was sometimes slightly sample-dependent. In any case, it was negligible compared with the intensity of the main Raman features occurring in the same spectral region. Here, reported spectra are plotted in arbitrary linear units, but they were scaled to each other in the hope of allowing qualitative comparison between the Raman features of the various samples.

3. Results

3.1. X-Ray Results

All samples dried at 170°C are composed of poorly crystallized boehmite (Fig. 1a), irrespective of the presence of alkali. In some cases, alkali-doped samples show diffraction peaks attributed to minor amounts of alkali nitrates. These salts may be formed from the neutralization of HNO_3, used to catalyze the hydrolysis of starting aluminates. Owing to their low decomposition temperature, some peaks of remarkable intensity disappear in samples treated at 400°C in which the boehmite phase is still dominant (Fig. 1b). At 170°C the average crystallite size of boehmite is found to be about 50 Å and is not affected by the presence of alkali.

The diffraction spectra of samples annealed at 600 and 800°C change noticeably with respect to those obtained at lower temperatures. The same crystalline structure and crystallization degree is observed for all systems (Figs. 1c and 1d). Phase identification is such as to suggest the formation of those Al_2O_3 phases usually referred to as transition aluminas (*15, 16, 19*) and previously studied by our group (*18*).

Samples annealed at 1000°C for 2 hr show a behavior dependent on the nature of the system. As shown in Fig. 2, the samples are not fully crystallized at this temperature either, making phase identification difficult. Nevertheless, the diffraction spectrum of pure alumina exhibits features typical of the Θ phase, with very weak peaks attributable

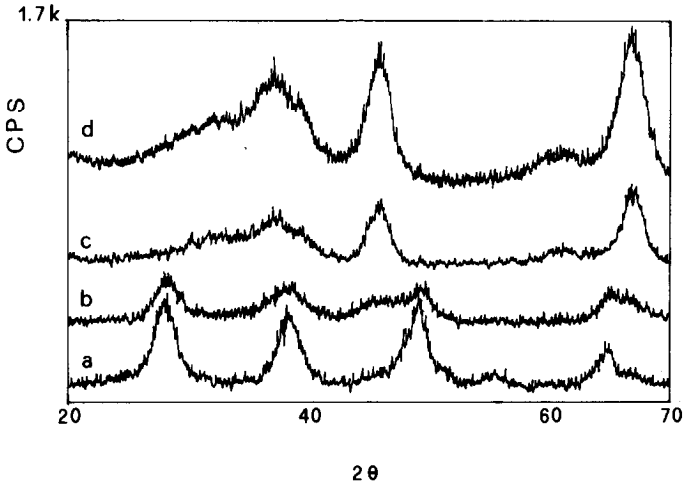

FIG. 1. Typical X-ray diffraction spectra of gel-derived samples of pure Al_2O_3 after treatment at various temperatures: (a) 170°C × 15 hr, (b) 400°C × 2 hr, (c) 600°C × 2 hr, (d) 800°C × 2 hr. See text for experimental conditions.

to α-alumina (Fig. 2c). On the other hand, the alkali-containing compounds give spectra mostly related with η-Al_2O_3, with minor β phase (Figs. 2a and 2b).

At 1200°C, pure alumina is completely transformed into the α-phase, and the sodium-enriched sample is composed of α- and β + β''-aluminas (Fig. 3), whereas in the potassium counterpart the β''-alumina phase was mainly present (Fig. 4). The presence of α-Al_2O_3 in the sodium-containing sample indicates alkali oxide release above 1200°C: indeed, for sodium-loaded alumina, the presence of α-Al_2O_3 increases upon prolonged heating. The X-ray spectra of Figs. 1–3 were recorded on samples

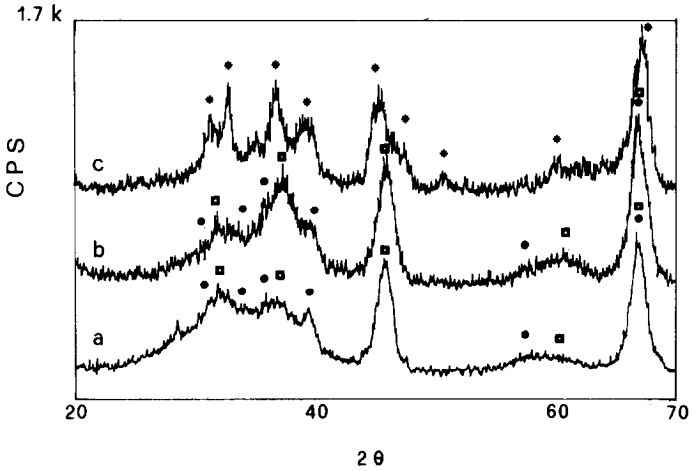

FIG. 2. X-ray diffraction spectra of samples treated at 1000°C × 2 hr. Patterns a and b obtained from potassium- and sodium-enriched samples, respectively: in both spectra, square marks indicate peaks of η-Al_2O_3; dots indicate β-phase peaks. In pure alumina spectrum c, stars indicate Θ-Al_2O_3 peaks.

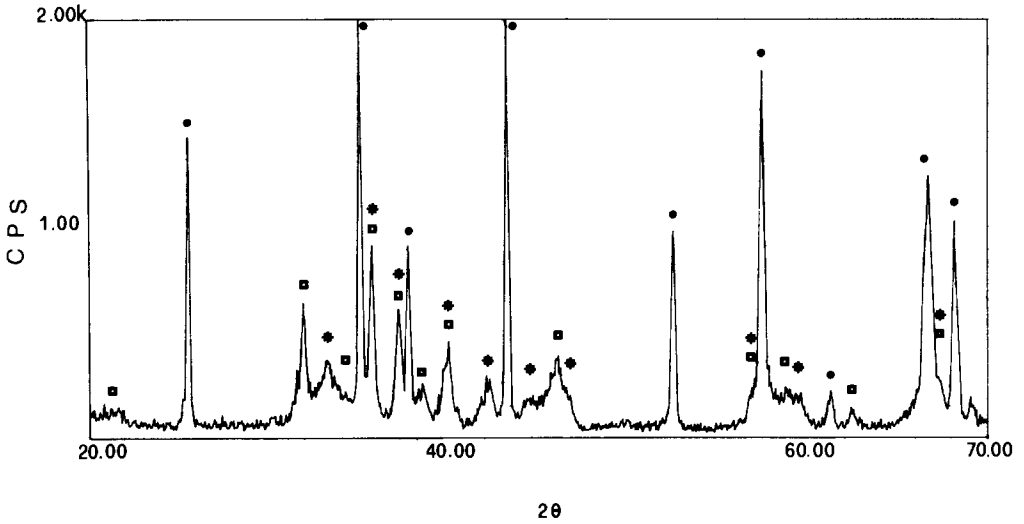

FIG. 3. X-ray diffraction spectrum of sodium-enriched sample treated at 1200°C × 2 hr; three different phases are identified: α-Al_2O_3 (dots), β-Al_2O_3 (stars), and β''-Al_2O_3 (squares).

powdered before heating and this fact may favor alkali oxide release during $\beta + \beta''$-Al_2O_3 formation, particularly for Na_2O which displays the highest vapor pressure. As for the precise assignment to β- and/or β''-alumina, the extensive overlap between peaks prevents attribution to a definite phase(s). Thus, as reported by Schmid (*33*), the quite similar patterns of the X-ray spectra of these phases, without any characteristic peaks, complicate assignment to either β- or β''-Al_2O_3.

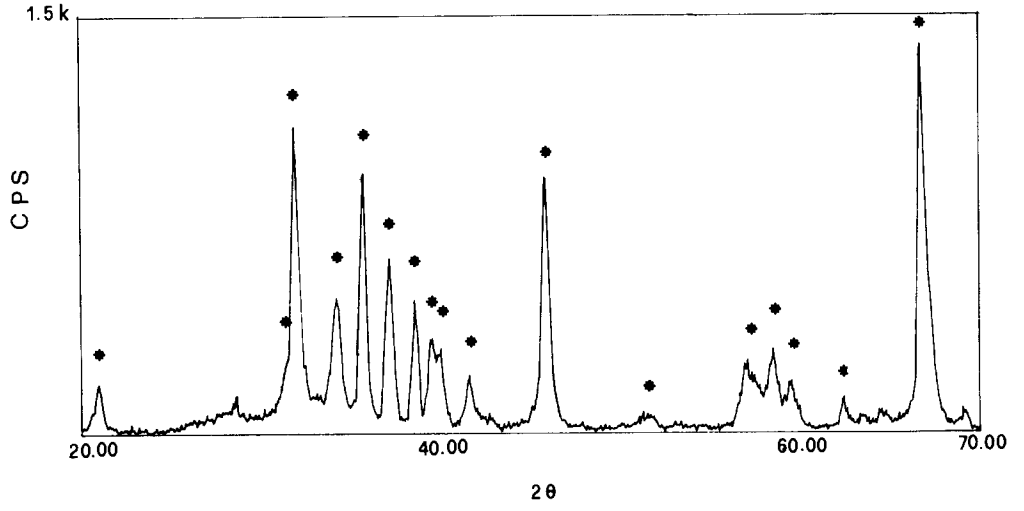

FIG. 4. X-ray diffraction spectrum of potassium-loaded sample treated at 1200°C × 2 hr; stars indicate β''-Al_2O_3 peaks.

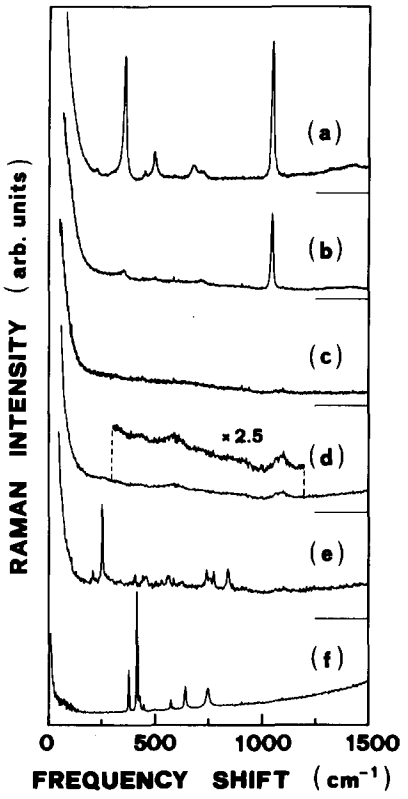

FIG. 5. Experimental Raman spectra obtained at room temperature under excitation of 514.5-nm line from pure Al_2O_3 samples treated at six different temperatures: (a) 170°C × 15 hr, (b) 400°C × 2 hr, (c) 600°C × 2 hr, (d) 800°C × 2 hr, (e) 1000°C × 2 hr, and (f) 1200°C × 2 hr. Part of spectrum d (between 300 and 1200 cm^{-1}) is also plotted on an expanded scale.

3.2. Raman Results

3.2.1. Experimental Spectra of Thermally Treated Boehmite Gels

Experimental Raman spectra of gel-derived boehmite samples, heated at six temperatures, are plotted in Fig. 5. The spectral intensity of each sample is quite good, as may be inferred from the signal-to-noise ratios. A low frequency, rapidly decreasing contribution and extending up to about 200 cm^{-1}, appears quite strong in all the reported spectra, except at the highest temperature treatment.

The spectrum from sample heated at 170°C (Fig. 5a) shows the features typical of polycrystalline boehmite (*35*), with very well-defined bands peaking at 369 and 1053 cm^{-1}. These peaks merge up from a relatively weak luminescence background, lying nearly flat up to about 2000 cm^{-1}. Moreover, less intense bands occur between 200 and 1200 cm^{-1}, complying with the observations of Kiss *et al.* (*35*). Finally, the two weak broad bands at about 1400 cm^{-1} can be attributed to methyl group vibrations (*36*), indicating that some moieties survived the gelling process.

The spectrum obtained after thermal treatment at 400°C (Fig. 5b) shows a strongly reduced Raman intensity, as regards the normal modes of highly distorted octahedral units of pseudo-boehmite. This effect is particularly evident for the 369 cm^{-1} peak intensity as well as for the 467-, 495-, and 720-cm^{-1} peaks, which are related to the A_{1g} and T_{2g} modes of the octahedra (*35*). On the other hand, Raman intensity related to OH^- defect modes (i.e., mode γOH at 733 cm^{-1}, mode δ_sOH at 1053 cm^{-1}, and mode γ_{as}OH at about 1110 cm^{-1}) undergoes minor changes with respect to the gel heated at 170°C for 15 hr. However, the intensity decrease of these OH^- defect modes suggests that some dehydration has already occurred in our samples at 400°C. Moreover, the persistence of weak features at about 1400 cm^{-1} reveals that the evaporation process of the organic solvent was not completed.

Spectra of samples heated at 600 and 800°C (Figs. 5c and 5d) look quite similar, showing only a rapidly decreasing leading edge in the low energy region, and a more slowly decreasing contribution extending up to about 1000 cm^{-1}. The most remarkable difference between the two spectra concerns the relative intensity of the OH^- defect modes in the region 1000–1200 cm^{-1}, which indicates different residual content of water in the two samples. Looking more

carefully at the spectrum between 200 and 1000 cm^{-1}, the occurrence of quite weak features merging up from the continuum is noteworthy: in samples treated at 800°C, where this phenomenon is more evident, they are observed at about 450, 600, and 800 cm^{-1}. Such spectral structures must be related to the presence of one or more alumina transition phases, although more specific insight is not possible on the basis of our Raman data.

Finally, as regards comparisons with samples heated at lower temperatures, quenching of Raman intensity from the vibrational modes of octahedral units, present in the boehmite structure, seems to be complete after treatment at these temperatures. This behavior supports the hypothesis that the intensity decrease depends on the kinetics of phase transformation.

A different situation occurs in the spectrum obtained from the 1000°C sample (Fig. 5e), which shows several new well-shaped features, although of rather low intensity. A relatively stronger, narrow peak is observed at 252 cm^{-1} with some other minor features at about 460, 565, 630, and 845 cm^{-1}, respectively. Moreover, a three-peaked feature is present in the region 740–780 cm^{-1}. The overall spectrum provides evidence for the formation at this temperature of different crystalline phases. As a matter of fact, none of the above-mentioned peaks fit those typical of the α-alumina phase (*37*), detected by X-ray analysis at this temperature; rather they correspond to Raman peaks reported for the Θ-alumina phase (*24*). Indeed, doubts may arise regarding the correspondence of the strongest peak, observed by us at 252 cm^{-1}, to that reported in Ref. (*24*) at 270 cm^{-1}: the immediate explanation of this disagreement is of an experimental nature, since the poorer resolution and lower intensity of the spectrum reported in Ref. (*24*) may have resulted in the convolution of such a peak with a laser plasma line, which we resolve at 267 cm^{-1}.

Last, the spectrum of sample treated at 1200°C (Fig. 5f) turns out definitely to be that of polycrystalline α-alumina with all the peaks expected for an unoriented but well-crystallized system (*37*). It looks particularly intense, with a flat background, slightly increasing in intensity at high wavenumbers (red shifted region), and definitely related to the luminescence centers, present as impurities in our α-Al_2O_3 compounds.

3.2.2. Experimental Spectra of Sodium- and Potassium-Enriched Samples

Figures 6 and 7 report two sets of Raman spectra of alkali-containing gels obtained after treatments at six different tempera-

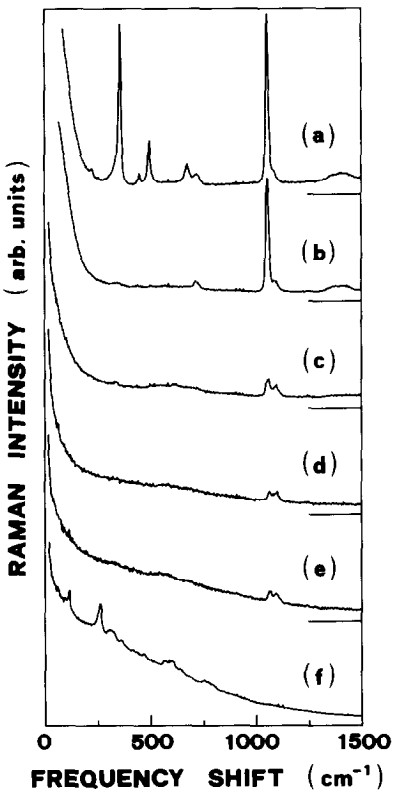

FIG. 6. As in legend to Fig. 5 but for sodium-enriched samples.

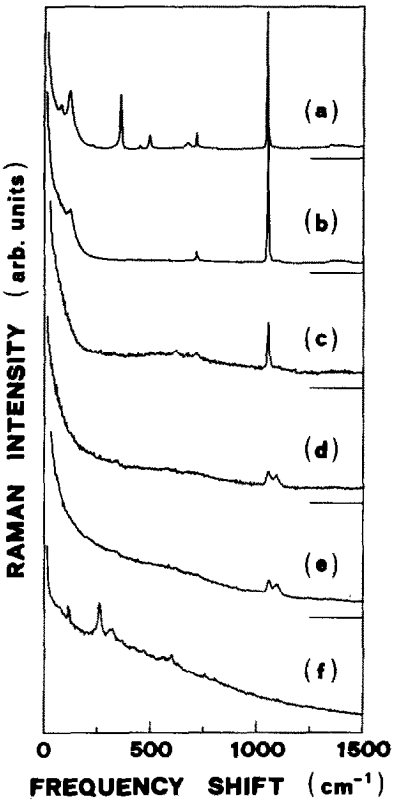

FIG. 7. As in legend to Fig. 5 but for potassium-containing samples.

tures. The spectrum of sodium-enriched sample, treated at 170°C for 15 hr, looks practically the same as that of pure pseudo-boehmite (see Fig. 5a). Instead, the spectrum of the potassium-containing sample presents some additional well-shaped peaks in the low-frequency region (about 85 and 125 cm^{-1}). They are certainly related to the presence of KNO_3: in fact, the Raman spectrum recorded at 160°C from this compound shows two E_g modes at 81 and 120 cm^{-1} (*38*). Furthermore, the overall spectral intensity turns out to be relatively stronger, probably related to the presence in the parent gel of highly polarizable K^+ ions which could enhance the electric-dipole fluctuations associated with the different vibrational modes of AlO_6 units. Indeed, the widths of the major Raman lines of the pseudo-boehmite component of the system are much narrower than in pure pseudo-boehmite and in the sodium-enriched Al_2O_3 system (as a matter of fact, Raman bandwidths are nearly halved in this case), suggesting a more uniform arrangement of K^+ ions in the mixed system. Moreover, the narrowing of the δ_sOH mode bandwidth indicates that K^+ ions also induce some ordering effect on the arrangement of water molecules in the host matrix.

Spectra of samples of both the sodium- and potassium-enriched Al_2O_3 systems, heated to 800°C (Figs. 6b–6d and 7b–7d), evolve in the same way as pure Al_2O_3; this fact indicates that, in all these systems, thermal annealing induces the formation of quite similar transition alumina phases. A slight difference is shown by the potassium compounds: in their spectra the higher intensity of the OH^- related bands above 1000 cm^{-1} reveals stronger retention of water. In addition the very broad feature centered around 600 cm^{-1} seems more pronounced with respect to the slowly decreasing continuum.

At 1000°C a clear difference in the reaction paths between the pure boehmite and the alkali-enriched materials is observed. The Raman spectra of the latter compositions do not show the well-shaped structures observed in pure alumina (see Fig. 5e) and related to the occurrence of the Θ-phase; they therefore reflect the absence of any remarkable structural change with respect to samples of the same original composition but treated at lower temperatures.

This different behavior is also more evident for the sodium- and potassium-containing mixtures treated at 1200°C: they unambiguously indicate the formation of β + β''-alumina phases, revealed by the presence of typical spectral fingerprints, like the strong peak occurring at 255 cm^{-1}, which is associated to the symmetric stretching

mode of the Al–O–Al bridge between two adjacent spinel blocks (*39*). In fact, all the main features present in the Raman spectrum of a pellet of sodium $\beta + \beta''$-alumina, obtained by solid state reaction of α-Al_2O_3 with Na_2CO_3, also appear in the spectra of our samples, obtained by thermal treatment of sodium-containing gels.

4. Interpretation and Discussion

Our Raman spectrum from pseudo-boehmite gel heated at 170°C perfectly fits the results obtained by Kiss *et al.* (*35*) from powdered boehmite, but it is superimposed upon a very flat background which allows much more reliable determination of both the frequency and relative intensity of the different Raman modes. In particular, the bands peaking at 733 and 1053 cm^{-1}, which are connected with the defective modes γOH and δ_sOH, show higher relative intensities when compared with that peaking at 369 cm^{-1}. This ratio may give a rough evaluation of the water content in our samples, which is higher than in polycrystalline boehmite, as expected after the exhaustive hydrolysis performed to obtain the gels. This fact is unambiguously demonstrated by the X-ray spectrum of Fig. 1a.

The apparent independence of Raman and XRD spectra of alkali content deserves comment: considering that we measure average crystallite dimensions of about 50 Å for all pseudo-boehmite samples at 170°C, the identity of spectral features, disregarding contribution of alkali nitrates, suggests that alkali loading is restricted to the surface of a pseudo-boehmite phase or intergranular volumes, i.e., zones with more H_2O and/or OH^- groups not engaged in a rigid crystalline framework. Thus, K^+- and Na^+-ion contents probably escape both XRD and Raman analysis. On the other hand, these speculations agree with the proposed nematic space organization of boehmite platelets (*15*), leaving enough free volume for nonordered localization of alkali cations.

Heat treatment at 400°C deeply affects the structure of pseudo-boehmite, as shown by the X-ray spectrum of Fig. 1b: this evolution has been previously studied (*18*) and is well-documented in the literature (*17, 19, 24*). The dehydroxylation process occurs even during the first thermal treatment at 400°C, as may be deduced by the relatively smaller intensity of the OH^- defect modes. As for pure $Al_2O_3 \cdot nH_2O$, the observed reduction of Raman intensity confirms that the original pseudo-boehmite structure has been lost. On the other hand, this transformation must involve symmetrization of those local arrangements typical of boehmite structure: in the material treated at 400°C, most of the octahedral groups around the Al^{3+} ion become nearly symmetric. Such a condition may be reached through transition to the γ phase of alumina (*13, 24*), which exhibits a defective spinel structure (*14, 15*).

Spinel structure is typical of an entire family of oxide materials with the general formula A_2BO_4, in which A^{3+} ions are octahedrally coordinated to O^{2-} ions, while B^{2+} ions have tetrahedral coordination with anions. γ-Al_2O_3 has a tetragonally distorted defective spinel structure, with two formula units ($Al_{2.66}\square_{0.33}O_4$) per rhombohedral unit cell (*14*). In this structure the cation vacancies are assumed to be disordered among the octahedral and tetrahedral sites (*14*), although preferential occupation of the tetrahedral sites has been proposed (*15*). Actually, whichever model is assumed for the distribution of these vacancies, the number of Al^{3+} ions in octahedral sites is greater by a factor between 2 and 3 than that of Al^{3+} in tetrahedral sites. These structural considerations may help in accounting for the reduced intensity of the Raman spectrum of sample heated at 400°C. In fact, the previous symmetry assignment of the vibrational modes for the regular spinel structure

A_2BO_4, developed within molecular group approximation, shows that the only Raman-active vibrations are the "internal modes" of the tetrahedral BO_4 group; octahedral group vibrations are not Raman-active (*40*). As a consequence of the above considerations, in γ-Al_2O_3, the number of Raman active groups (Al^{3+} ions tetrahedrally coordinated to the oxygens) is a minor fraction of the inactive ones, and this fact cannot be neglected when weak Raman intensity is considered. Moreover, the disordered distribution of the cation vacancies over the tetrahedral sites, as revealed by streaking in the characteristic X-ray reflections (*41*), may also account for the broadened shape of the observed weak Raman structures, which seem to reflect a vibrational density of states. Besides positional disorder on the atomic scale and its effects on the Raman spectra, such a system, as well as the samples treated at higher temperatures (600 and 800°C), is disordered and inhomogeneous on a more extended scale. This is evident from the X-ray spectral features of Figs. 1c and 1d: the dehydroxylation process occurring more quickly above 400°C results in the formation of transitional alumina structures, among which the δ-Al_2O_3 phase can certainly be attributed (*14–16*). The presence of Na^+ and K^+ ions does not affect the spectral features, so that it can be argued that metastable phase occurrence only induces topotactical arrangements of pseudoboehmite; thus, the external presence of alkali is ineffective for the low-temperature appearance of phases like α-Al_2O_3 or β-Al_2O_3, which requires hexagonal anion organization with high activation energy.

For pure alumina material, interesting evolution is revealed by the Raman spectrum of the 1000°C sample (Fig. 5e), which shows several new well-shaped features. The overall spectrum gives evidence for the formation, at this temperature, of new well-defined crystalline phases, as detected by previous X-ray diffraction studies (*10, 15, 16, 19*). The reported transition phase is the monoclinic Θ phase. Its low-symmetry spatial group may explain the occurrence of several Raman-active modes, in contrast to the other phases, produced by heating at lower temperatures, which possess more symmetric structures. The frequency difference observed for the highest intensity peak (252 cm^{-1}), with respect to the previous Raman study on alumina transition phases (270 cm^{-1}) (*24*), has already been discussed. If we discard the banal explanation based on experimental considerations, the difference in energy of this peak may be related to the different arrangement of the oscillating ion groups in the resulting crystalline mixture. Indeed, in Ref. (*24*), the Θ phase is reported to be mixed with the γ or α phase depending on heat treatment. Therefore, in particular conditions (kinetics and crystalline order), the samples may be characterized by different stress distribution, or by slightly modified aggregation of basic units, as suggested by the energy difference, 252 vs 270 cm^{-1}. Finally, it is of interest to note the correspondence of the 252 cm^{-1} mode with the A_{1g} mode of about the same frequency observed in the β-aluminates, which corresponds to the compressional motion of heavy Al_2O_3 units (spinel blocks) against the bridging oxygen (*39*). This fact does not imply formation of β-like crystalline structures, but rather the formation, during phase-rearrangement, of quite open atomic configurations with similar bridged aggregates.

The systems at 1000°C are still not fully crystallized: the X-ray data for pure Al_2O_3 show the presence of a minor amount of α-Al_2O_3, whereas the Raman spectrum does not show signals associated with this phase. Since the formation of corundum is highly energy-demanding, the fine powder morphology of samples heated at 1000°C and analyzed by X-ray may have favored the appearance of α-Al_2O_3 crystallites at the grain surface.

Concerning the nature of the disorder changes after heating above 1000°C, both Raman spectrum and X-ray diffraction patterns of sample at 1200°C show well-defined peaks, usually associated with the occurrence of crystalline order over a significant scale. The expected collapse of Θ-Al_2O_3 to α-Al_2O_3 and of alkali-loaded aluminas to $\beta + \beta''$-Al_2O_3 is already evident from from X-ray spectra of Figs. 3 and 4, as well as from the change in the Raman spectra of Figs. 5–7.

In conclusion, with the aim of avoiding boehmite formation by gelling, grains of pure Al_2O_3 heated at 1000°C might be used for seeding an aluminum alkoxide solution with substoichiometric water. The relatively open structure of the material at 1000°C may also allow diffusion of alkali ions, yelding $\beta + \beta''$-alumina from Θ-Al_2O_3; as a matter of fact, the potential advantage of the preparation of ion-conductive β-alumina from alkali and aluminum alkoxide solutions is severely restricted by primary separation of pseudo-boehmite.

Acknowledgments

The authors are indebted to Dr. Chiara Schmid who furnished them with the pellet of $\beta + \beta''$-alumina used as standard. This work was partially funded by the Consiglio Nazionale delle Ricerche under Contract 87.02240.59 and by SNIA FIBRE spa (Milano).

References

1. R. Collongues, D. Gourier, A. Kahan, J. P. Boilot, Ph. Colomban, and A. Wicker, *J. Chem. Phys. Solids* **45,** 981 (1984); and references therein.
2. J. L. Sudworth and A. R. Tilley, "The Sodium Sulfur Battery," Chapman & Hall, London (1985).
3. J. L. Briant and G. C. Farrington, *J. Solid State Chem.* **33,** 385 (1980).
4. G. K. Duncan and A. R. West, *Solid State Ionics* **9/10,** 259 (1983).
5. J. D. Hodge, *Ceram. Bull.* **62,** 244 (1983).
6. B. E. Yoldas and D. P. Partlow, *Amer. Ceram. Soc. Bull.* **59,** 640 (1980).
7. S. Yamaguchi, K. Terabe, and Y. Iguchi, *Solid State Ionics* **25,** 171 (1987).
8. L. G. Klein, "Sol-Gel Technology for Thin Films, Fibers, Preforms, Electronics and Specialty Shapes," Noyes Press, Park Ridge, NJ (1988).
9. T. Max and S. Sakka, *J. Non-Cryst. Solids* **100,** 303 (1988).
10. B. C. Lippens and J. H. de Boer, *Acta Crystallogr.* **17,** 1312 (1964).
11. H. Yanagida, G. Yamaguchi, and J. Kubota, *Bull. Chem. Soc. Japan* **38,** 2194 (1965).
12. P. Boch, D. Fargeot, C. Gault, and F. Platon, *Rev. Int. Hautes Temp. Refract.* **1,** 18 (1981).
13. A. C. Pierre and D. R. Uhlmann, *J. Non-Cryst. Solids* **82,** 271 (1986).
14. M. I. Baraton and P. Quintard, *J. Mol. Struct.* **79,** 337 (1982).
15. X. Yang, A. C. Pierre, and D. R. Uhlmann, *J. Non-Cryst. Solids* **100,** 371 (1988).
16. A. van Zyl, Ph.D. Thesis, University of Cape Town (1987); and A. van Zyl, *in* "Proceedings the International Seminar on Solid State Ionics Devices" (B. V. R. Chowdari and S. Radhadkrishna, Eds.), p. 457, World Scientific, Singapore (1988).
17. M. Inoue, Y. Kondo, and T. Inui, *Inorg. Chem.* **27,** 215 (1988).
18. G. Carturan, R. Di Maggio, M. Montagna, O. Pilla, and P. Scardi, *J. Mater. Sci.*, in press.
19. Y. Hirai, T. Fukuda, Y. Kobayashi, H. Kuwahara, Y. Kido, and K. Kubota, *Solid State Commun.* **62,** 637 (1987).
20. W. A. Yarbrough and R. Roy, *J. Mater. Res.* **2,** 494 (1987).
21. M. Deflandre, *Bull. Soc. Fr. Mineral.* **55,** 140 (1932).
22. G. Ervin, *Acta Crystallogr.* **5,** 103 (1952).
23. M. Kunagai and G. L. Messing, *J. Amer. Ceram. Soc.* **68,** 500 (1985).
24. T. Assih, A. Ayral, M. Abenoza, and J. Phalippou, *J. Mater. Sci.* **23,** 3326 (1988).
25. A. Bertoluzza, C. Fagnano, M. A. Morelli, V. Gottardi, and M. Guglielmi, *J. Non-Cryst. Solids* **82,** 127 (1986).
26. C. A. M. Mulder and A. A. J. M. Damen, *J. Non-Cryst. Solids* **93,** 387 (1987).
27. G. Mariotto, M. Montagna, G. Viliani, R. Campostrini, and G. Carturan, *J. Phys. C* **21,** L797 (1988).
28. G. Mariotto, G. C. Farrington, and E. Cazzanelli, *in* "Transport–Structure Relations in Fast Ion and Mixed Conductors" (F. W. Poulsen, N. Hessel Andersen, K. Clausen, B. Skaarup, and O. Toft Sorensen, Eds.), p. 455, RISO National Laboratory, Roskilde (1985).

29. G. MARIOTTO AND G. C. FARRINGTON, *Solid State Ionics* **18/19,** 619 (1986).
30. M. CATTI, E. CAZZANELLI, G. IVALDI, AND G. MARIOTTO, *Phys. Rev. B* **36,** 9451 (1987).
31. B. E. YOLDAS, *Bull. Amer. Ceram. Soc.* **54,** 289 (1985).
32. International Center of Diffraction Data, 1605, Park Lane, Swarthmore, PA.
33. C. SCHMID, *J. Mater. Sci. Lett.* **5,** 263 (1986).
34. H. P. KLUG AND L. E. ALEXANDER, "X-Ray Diffraction Procedures," Wiley, New York (1974).
35. A. B. KISS, G. KERESZTURY, AND L. FARKAS, *Spectrochim. Acta A* **36,** 653 (1980).
36. N. B. COLTHUP, L. H. DALY, AND S. E. WIBERLEY, *in* "Introduction to Infrared and Raman Spectroscopy," Chap. 5, Academic Press, New York (1964).
37. S. P. PORTO AND R. S. KRISHNAN, *J. Chem. Phys.* **47,** 1009 (1967).
38. I. NAKAGAWA AND J. L. WALTER, *J. Chem. Phys.* **51,** 138 (1967).
39. PH. COLOMBAN AND G. LUCAZEAU, *J. Chem. Phys.* **72,** 1213 (1980).
40. W. B. WHITE AND B. A. DE ANGELIS, *Spectrochim. Acta A* **23,** 985 (1967).
41. S. J. WILSON, *J. Solid State Chem.* **30,** 247 (1979).